Canadian Technical Report of

Hydrography and Ocean Sciences No. 62

August 1985

DESIGN, CONSTRUCTION AND PERFORMANCE OF A MOORED STABLE PLATFORM

by

J. Fletcher[1], R.G. Mills[1], and S.D. Smith[2]

[1] Whitman, Benn and Associates Ltd.
5251 Duke St., Suite 212
Halifax, N.S. B3J 1N9

[2] Atlantic Oceanographic Laboratory
Ocean Science and Surveys, Atlantic
Department of Fisheries and Oceans
Bedford Institute of Oceanography
P.O. Box 1006
Dartmouth, N.S. B2Y 4A2

A C K N O W L E D G E M E N T S

We wish to thank the many people whose contribution made this work possible; in particular J. Brooke, J.-G. Dessureault, R.J. Anderson and D.L. Hendsbee for their assistance in the operation of the platform and retrieval of data, and J. Ritcy and B. Lohnes of Dominion Divers Ltd. for their assistance in the installation and inspection of the platform. Funding for the design, installation and operation of the tower was provided by the Department of Fisheries and Oceans, and interpretation and reporting of results was funded by the Office of Energy Research and Development of the Department of Energy, Mines and Resources, Canada.

Cat. No. FS 97-18/62E ISSN 0711-6764

Correct citation for this publication:

Fletcher, J., Mills, R.G., and Smith, S.D., 1985. Design, Construction and Performance of a Moored Stable Platform. Can. Tech. Rep. Hydrogr. Ocean Sci. 62 : iv + 41 p.

ABSTRACT

Fletcher, J., Mills, R.G., and Smith, S.D., 1985. Design, Construction and Performance of a Moored Stable Platform. Can. Tech. Rep. Hydrogr. Ocean Sci. 62 : iv + 41 p.

The design, construction and performance of a stable, moored platform are described. The platform was installed in 59 m of water at the approaches of Halifax harbour, N.S. Wave height, tower acceleration and mooring cable tensions were measured under storm conditions with unlimited fetch. The wave height and load values are compared with theoretical values calculated using steady-state (static) design methods, and the motion of the platform is discussed in relation to both the non-linearity of the mooring system and the dynamic response of the structure and moorings.

RÉSUMÉ

Fletcher, J., Mills, R.G., and Smith, S.D., 1985. Design, Construction and Performance of a Moored Stable Platform. Can. Tech. Rep. Hydrogr. Ocean Sci. 62 : iv + 41 p.

On décrit la conception, la construction et la performance d'une plate-forme amarrée stable. La plate-forme reposait dans 59 m d'eau aux approches du port d'Halifax (N.E.). On a mesuré la hauteur des vagues, l'accélération de la tour et la tension dans les câbles d'amarrage dans des conditions de tempête avec un fetch illimité. La hauteur des vagues et les charges mésurées on été comparées à des valeurs théoriques calculées à partir de maquettes à l'équilibre (statiques); on analyse le mouvement de la plate-forme en fonction de la non-linéarité du système d'amarrage et de la réponse dynamique de la structure et des amarres.

TABLE OF CONTENTS

DESIGN, CONSTRUCTION AND PERFORMANCE OF A MOORED STABLE PLATFORM

J. Fletcher, R.G. Mills

Whitman, Benn & Associates Ltd.,
5251 Duke St.,
Halifax, N.S.

and

Stuart D. Smith

Atlantic Oceanographic Laboratory
Bedford Institute of Oceanography
Dartmouth, N.S.

INTRODUCTION

In recent years, meteorologists and oceanographers have given increasing attention to the exchange of energy between air and sea, and its impact on global wind circulation and weather. The exchange mechanisms have been under study by the air-sea interaction group at the Bedford Institute of Oceanography (BIO) since the early 1960's, and have required the development of instruments capable of measuring turbulent fluctuations of wind velocity and air temperature (Dessureault and Knox, 1980, Smith 1980a) and the development of a support for the instruments which does not distort the measurements. Structures used to support these instruments have included bottom-resting platforms and floating platforms with as many as 13 mooring lines and anchors (Doe and Brooke, 1965; Mills, 1972). Various problems have been experienced with these systems, including the accurate placement of anchors, estimating the prevailing environmental conditions and limiting the yaw motion of the structure.

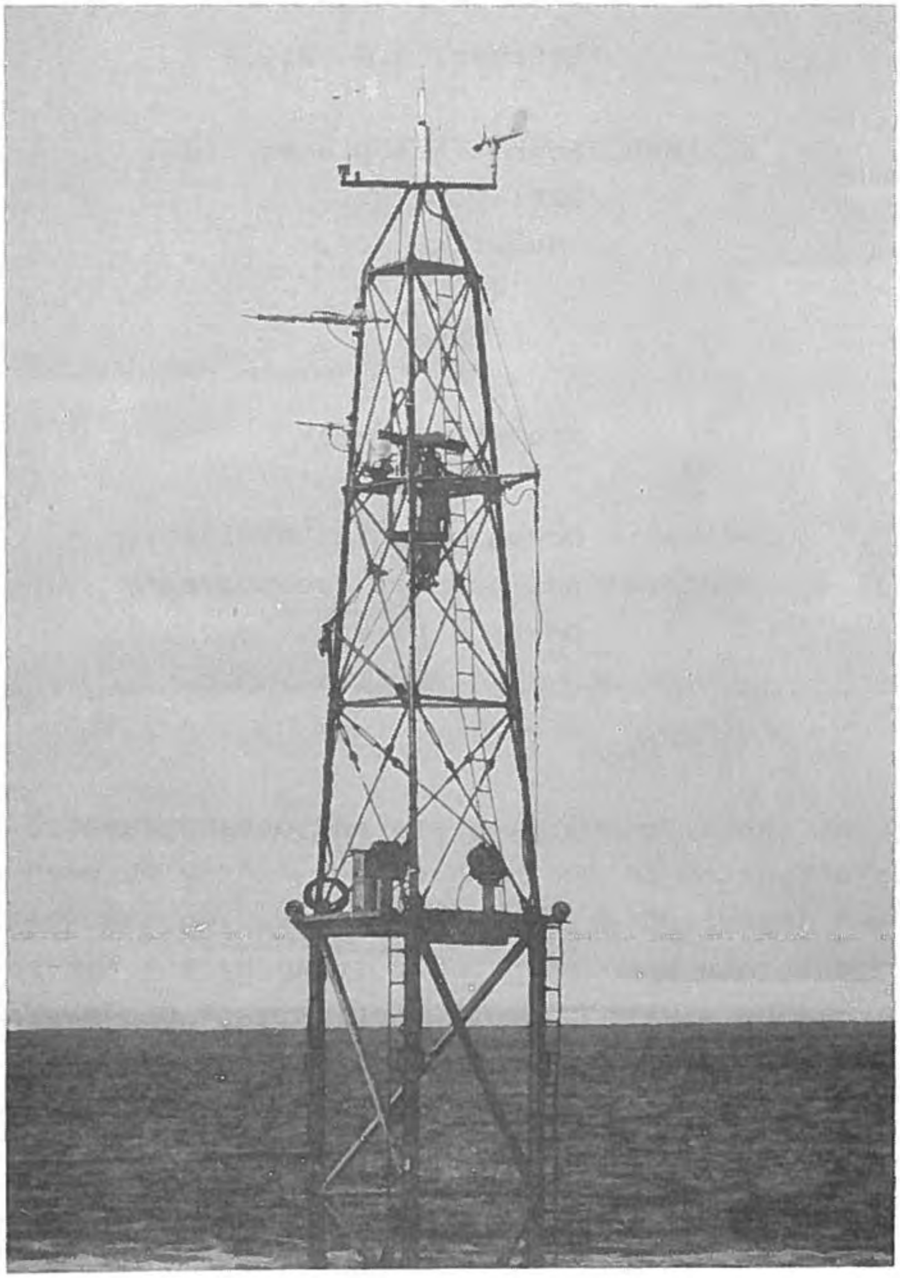

Fig. 1: The stable platform

The Mark IV Stable Platform (Fig. 1) was designed by Whitman, Benn and Associates Ltd. and fabricated for BIO by Stuart Industries Ltd., Fall River, N.S., and was operated between 1976 and 1978 as an unmanned recording station. It was moored 10 km from shore at the approaches to Halifax Harbour, with exposure to the full fetch of the North Atlantic for winds from the east and south. The water depth of 59 m allowed 10 s waves to travel at 99% of their deep water phase velocity (12 s waves, 96%); thus it was typically exposed to deep water waves.

The platform was equipped to measure tension in each of its six upper mooring cables, acceleration in three axes, wave height, tilt, wind velocity in three axes, air and sea temperatures and current velocity. A total of 192 data runs, consisting of a short calibration record followed by a continuous recording of 40 min. average duration, were made during the winters of 1976-77 and 1977-78. In each case, twelve channels of data were selected by radio link from the receiving station, and were transmitted simultaneously. The multiplexed signal was recorded on analog magnetic tape, displayed on a chart recorder and digitized (Smith, 1974). The statistical analysis of data included the computation of spectra and cross-spectra for the various channels (Dobson et al, 1974). While the major effort of the project was directed towards the collection and analysis of wind stress data (Smith, 1980b), the platform's performance was monitored during 30 engineering runs. Concurrent measurements of wave height, cable tensions and accelerations were taken, which provide real, continuous data for a wide range of sea states acting on a simply shaped structure.

PLATFORM DESIGN

The design of the platform was based on the requirement to support a thrust anemometer (Smith, 1980a, b, c) at a height of 13 m above mean sea level. Design constraints included the need to minimize the platform's wind blockage, minimize air flow distortion, and minimize movement of the platform.

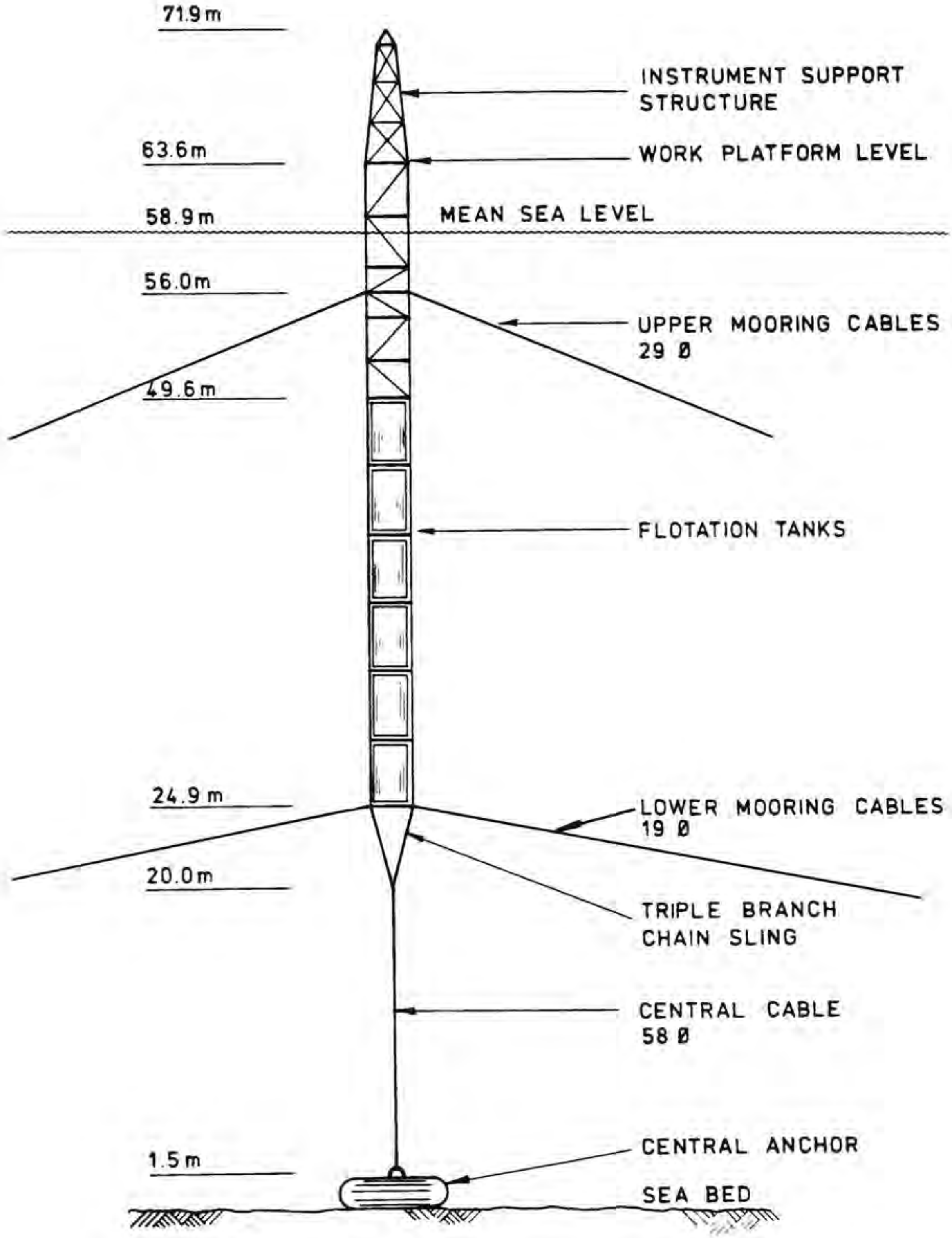

Fig. 2: Elevation of the platform tower

Platform Configuration: The platform consisted of a 47 m long tower (Fig. 2), a central mooring cable and anchor, and twelve radial mooring cables connected to the tower at two levels (Fig. 3). The tower weighed 250 kN (mass: 25.5 T) and displaced 594 kN (1 N = 0.102 kgf = 0.224 lb). It had a triangular cross-section framed in tubular members. The three main vertical members were 152 mm in diameter, spaced 1.83 m centre-to-centre, and enclosed six flotation tanks below the elevation of the extreme wave troughs. The exposed area was minimized directly above and below mean sea level, where wave induced water particle velocity is greatest. Typical values for the sectional width of the tower that were used in design load calculations were 0.46 m above elevation 63.6 m, 1.37 m below elevation 63.6 m and 2.29 m at the flotation tanks. Additional areas were included at the instrument and work platform levels.

Mooring configuration: The choice of mooring cables, their anchorage, and the initial cable tensions were the most critical factors to the economy and performance of the structure. The buoyancy of the tower was resisted by a 36.4 tonne central anchor on 20 m of cable, and lateral movement (surge, sway, pitch and roll) was restrained by six pairs of cables. Yaw was restricted by attaching the cables to the apexes of the triangular cross section. This provided a counterbalanced eccentricity of 0.4 m in each cable with respect to the vertical axis of the tower. Each pair of cables was anchored at the seabed by two 12 tonne concrete blocks; this configuration being selected to facilitate installation.

Environmental loads: The design loading was based on a 60 year peak-to-trough wave height of 18 m (Neu, 1971, 1982), a uniform current of 0.25 m s^{-1} and a wind speed of 45 m s^{-1}, all acting simultaneously. Various combinations of wave period and sea level were investigated using Stokes 3rd order wave theory (Skjelbreia, 1959). The mean current was added directly to the wave-induced particle velocity over the full height of the

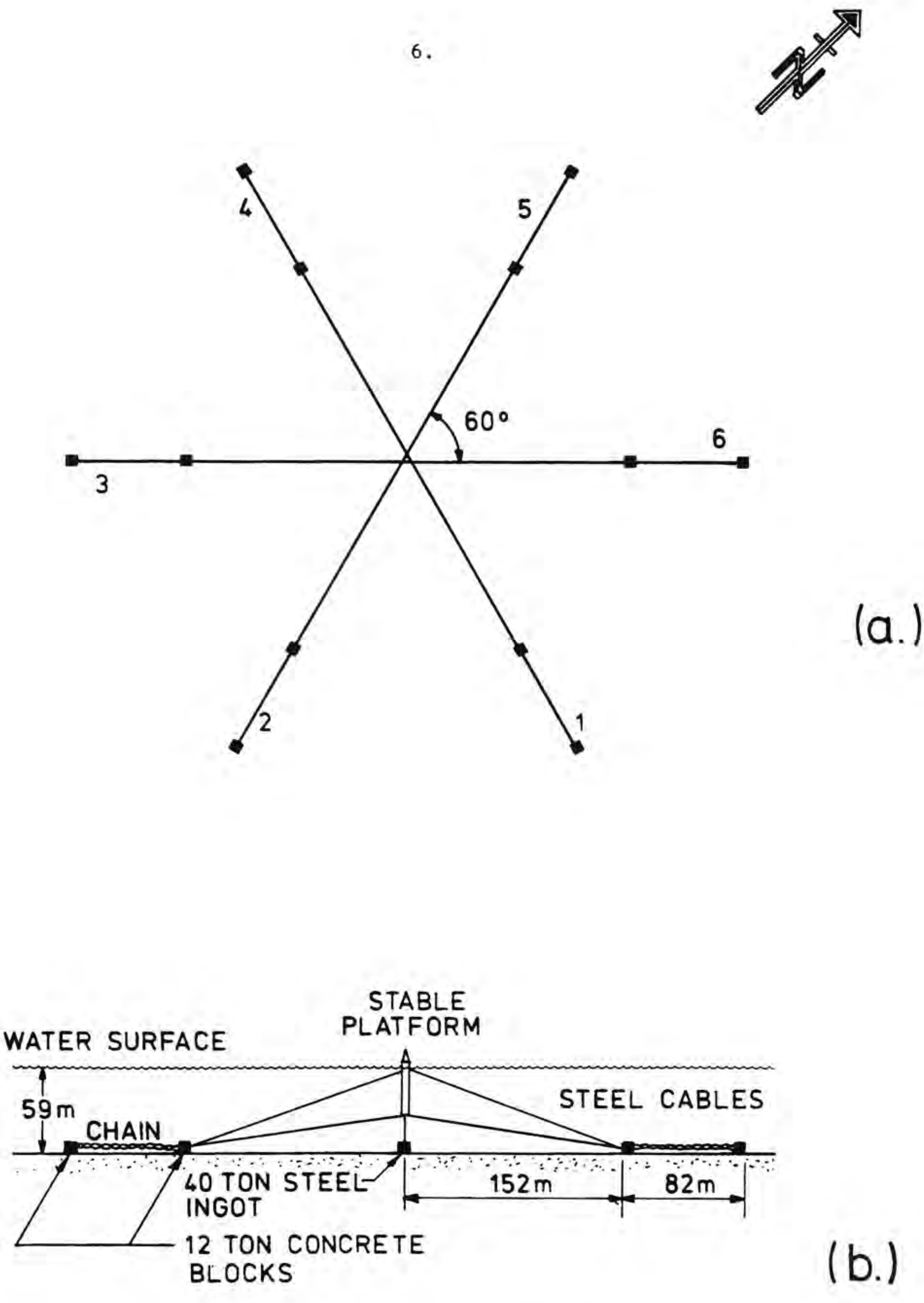

Fig. 3: Mooring of the platform, (a) plan, (b) section

submerged tower. Horizontal wave forces were calculated by Morison's equation (Morison et al, 1950):

$$F = 1/2 \rho C_d A v|v| + \rho C_m V \dot{v} \tag{1}$$

(See Notation, page 38). A drag coefficient value of C_d = 0.78 was used, based on recorded wave height and load data from previous installations. The inertia force was considerably smaller than, and 90° out of phase with, the drag force. An inertial coefficient value of C_m = 1.5 was used for design. In comprehensive reviews of Morison's equation and data on wave forces, Hobgen et al (1977) and Leonard et al (1981) described the coefficients C_d and C_m as functions of the dimensionless ratios of Reynold's Number, $R_e = vD/\nu$, and the Keulegan - Carpenter Number, $K = vT/D$, within the limits in physical scale for which Morison's equation is applicable.

Both R_e and K are proportional to wave height. Their values also vary with phase and are dependent on the elevation and cross-section of the element of the tower under consideration. In steady flow, the drag coefficient C_d is well correlated with R_e and is characterized by various conditions of the flow in the wake and in separation of the boundary layer. Published values for C_d in waves show a similar trend to that of the steady state condition in that C_d decreases considerably as R_e increases over the approximate range of 10^4 to 10^6. Average values derived from several studies indicate that C_d reduces from 1.2 to 0.6 (Hobgen et al, 1977) or less (Leonard et al, 1981) over this range for structures dominated by drag forces. For waves with a 10 s period applied to the Stable Platform, a Reynold's number of 10^6 is reached at the top of the buoyancy tank section when the wave height is 2.3 m whereas, because of the reduced diameter of the structural elements, the corresponding Reynold's number at mean sea level is 1.2×10^5. Waves in the order of 20 m would be required to attain

$R_e = 10^6$ at mean sea level. Although it is inexact to approximate a uniform value for C_d over the full height of the tower, the resulting uncertainty in results is small relative to the documented scatter of estimates of C_d.

The Keulegan - Carpenter number K is a measure of the relative importance of drag and inertia forces. Values in the order of five or less indicate inertia dominance, with the coefficient of inertia C_m close to its theoretical value of 2.0 for inviscid flow. Values greater than 25 indicate drag dominance. The transition zone between 5 and 25 contains a wide scatter of experimental results. Leonard et al (1981) suggest a C_m value of 1.5; however, experimental results are mainly confined to recordings under predominantly drag loading conditions. Also, experimental results (Chakrabarti, 1981) indicate the drag forces for this range are particularly susceptible to the degree of surface roughness due to marine fouling. At the top of the buoyancy tanks, the Keulegan - Carpenter number reached 25 for wave heights in excess of 5.0 m. The design value of $C_m = 1.5$ and the dominance of drag forces at design loading are therefore consistent with the published data. K reduces as smaller wave heights and lower elevations of the buoyancy tank section of the tower are considered, and increases sharply above the buoyancy tanks due to the reduction in cross-sectional area.

Analysis for design: The tower and moorings were modelled as a pin-jointed space frame of discrete rod elements with forces applied at the nodal points and restraint provided at the anchor end of the cable elements. A static, linear-elastic analysis was performed for stress and displacement. A static, non-linear displacement analysis was subsequently performed (Mills, 1979), using a series of hinged rod elements to model each cable.

INSTALLATION AND OPERATION

Installation: The anchor blocks, the connecting chain, the pendant line from the inner anchor and the buoys were assembled for each leg of the anchor layout. Using a floating crane, a tug and radio positioning equipment, each outer anchor was released approximately 60 m outside its designated position. The inner block was dragged off the barge and dropped as the crane moved towards the centre of the anchor layout, when the chain connecting it to the outer anchor became taut. The anchors were then dragged into position using a tow line from the crane to the pendant line on the inner block.

To position the tower in the centre of the anchor layout, the tower and central anchor were first deployed near their final position. Temporary cables were then attached to four of the six pendant lines on the inner anchors and these cables were run through sheaves at the tower base up to winches on the tower platform. The buoyancy of the tower was then increased to float the central anchor, and the tower was positioned by adjusting the lengths of the temporary cables. Once the tower was in the correct position, the flotation tanks were ballasted and the central anchor was set on the sea floor. Permanent cables were later measured, attached, tightened by winch and permanently secured. Due to lack of adjustment in the permanent cable assemblies, it was impossible to tension the cables to their design values prior to the onset of the first winter season. The platform was inspected periodically; upper cable tensions were monitored and, after one season in service, cable tensions were increased to 9.9 kN. Ballast water was added to the lower tanks so that the net buoyancy was reduced to 137 kN, excluding cable loads, resulting in an "at rest" tension of 95 kN in the central mooring cable.

Instrumentation: In addition to sensors for air-sea interaction studies, sensors were mounted on the platform to collect engineering data for the following purposes:

Table 1 Summary of engineering data runs from stable platform

Start Time GMT	Date	Run No.	Wind speed m/s	Dir'n from deg.	RMS waves m	RMS tension (KN) 1	2	3	4	5	6	rms accel. m/s^2
1342	21/10/76	12	20	135	1.30	3.1	4.7	1.2	---	2.8	---	0.38
1308	03/12/76	28	16	276	0.60	0.3	0.3	0.4	---	0.3	0.4	0.20
1824	15/03/77	50	17	071	0.94	0.9	---	0.4	---	---	---	0.33
1622	23/03/77	56	20	090	---	---	---	---	---	---	---	---
1357	04/04/77	72	15	315	---	---	---	---	---	---	---	---
0600	06/04/77	75	16	203	---	---	---	---	---	---	---	---
0813	06/04/77	77	14	225	---	---	---	---	---	---	---	---
1535	10/11/77	88	6	126	0.44	0.4	---	0.5	0.4	0.5	0.4	0.09
1140	14/11/77	91	7	270	0.56	0.9	---	0.7	1.0	0.9	0.6	0.10
1138	18/11/77	96	16	222	0.93	0.7	---	2.3	1.7	1.0	1.1	0.18
1502	18/11/77	99	10	223	0.81	1.7	---	2.5	1.4	1.5	1.8	1.16
1639	24/11/77	106	8	122	0.65	0.8	---	0.5	0.7	0.6	0.5	0.14
1659	26/11/77	111	8	108	0.96	3.5	---	0.8	1.5	1.6	5.0	0.18
1305	27/11/77	114	19	245	1.22	1.4	---	3.5	2.8	2.4	2.2	0.21
1700	27/11/77	118	19	256	1.37	1.1	---	6.0	4.2	4.0	2.1	0.22
2103	27/11/77	122	16	271	1.14	1.1	---	4.4	3.0	3.3	2.0	0.19
1149	28/11/77	127	6	291	0.76	0.8	---	---	1.0	1.5	1.5	0.13
1540	09/01/78	137	17	147	0.97	---	---	---	1.4	1.0	0.9	0.18
0035	10/01/78	142	20	148	1.46	2.7	---	---	2.2	2.5	2.4	0.25
0242	10/01/78	144	15	195	1.69	3.3	---	---	3.3	3.6	2.2	0.28
1126	10/01/78	149	16	231	1.87	2.6	---	---	3.6	6.4	4.7	0.56
1322	11/01/78	155	7	288	0.74	0.6	---	---	0.9	0.7	1.1	0.13
2039	14/01/78	165	15	175	1.88	6.3	---	---	5.5	5.2	3.0	0.35
0247	15/01/78	168	17	166	1.16	1.3	---	---	1.0	0.9	1.1	0.20
0550	15/01/78	171	17	159	1.34	1.6	---	---	1.5	1.1	1.5	0.23
1246	18/01/78	173	14	101	0.62	0.9	---	---	0.6	0.6	0.7	0.16
1904	18/01/78	174	11	109	1.05	1.8	---	---	1.0	0.8	1.2	0.20
0036	19/01/78	177	11	221	0.92	1.0	---	---	1.3	---	1.0	0.18
1742	26/01/78	180	15	181	0.80	0.6	---	---	0.7	---	---	0.21
1314	27/01/78	183	12	220	1.18	0.8	---	---	1.3	---	---	0.17

1) to monitor the structural integrity of the platform and to determine the platform's influence on the accuracy of scientific measurements,

2) to measure wave height and structural loading, and

3) to investigate the dynamic behaviour of the platform.

The instrumentation on the platform relevant to engineering analysis included a wavestaff, an anemometer, three accelerometers mounted orthogonally (east, north, and vertical), and a tension sensor (load cell) in each of the upper mooring cables. A telemetry system (Dinn, 1973) transmitted the data in FM multiplexed form to a control and receiving station at the Bedford Institute of Oceanography. The remote system was powered by a 36 V DC battery supply which was mounted at the work platform level and charged by a 25W Aerowatt windmill generator.

The 12 m wavestaff, manufactured by the Nova Scotia Research Foundation, consisted of a flexible plastic tube grooved and wound with two lengths of exposed wire. The electrical resistance of the portion of the wires above the water was measured, providing an accurate measurement of wave height limited only by the range of the wavestaff and by possible vertical movement or tilt of the tower. The upper limit of wave height measurement was generally in the order of 10 m peak-to-trough due to tidal variations.

The accelerometers, mounted at the top of the tower, were controlled to transmit data over either of two sets of scale ranges: ± 0.02 g (vertical) and ± 0.1 g (horizontal), or ± 0.1 g (vertical) and $\pm$ 0.5 g (horizontal). For the most part, the smaller ranges proved to be sufficient. However, with the accelerometer fixed relative to the platform, inaccuracies in acceleration measurements were possible, particularly in the

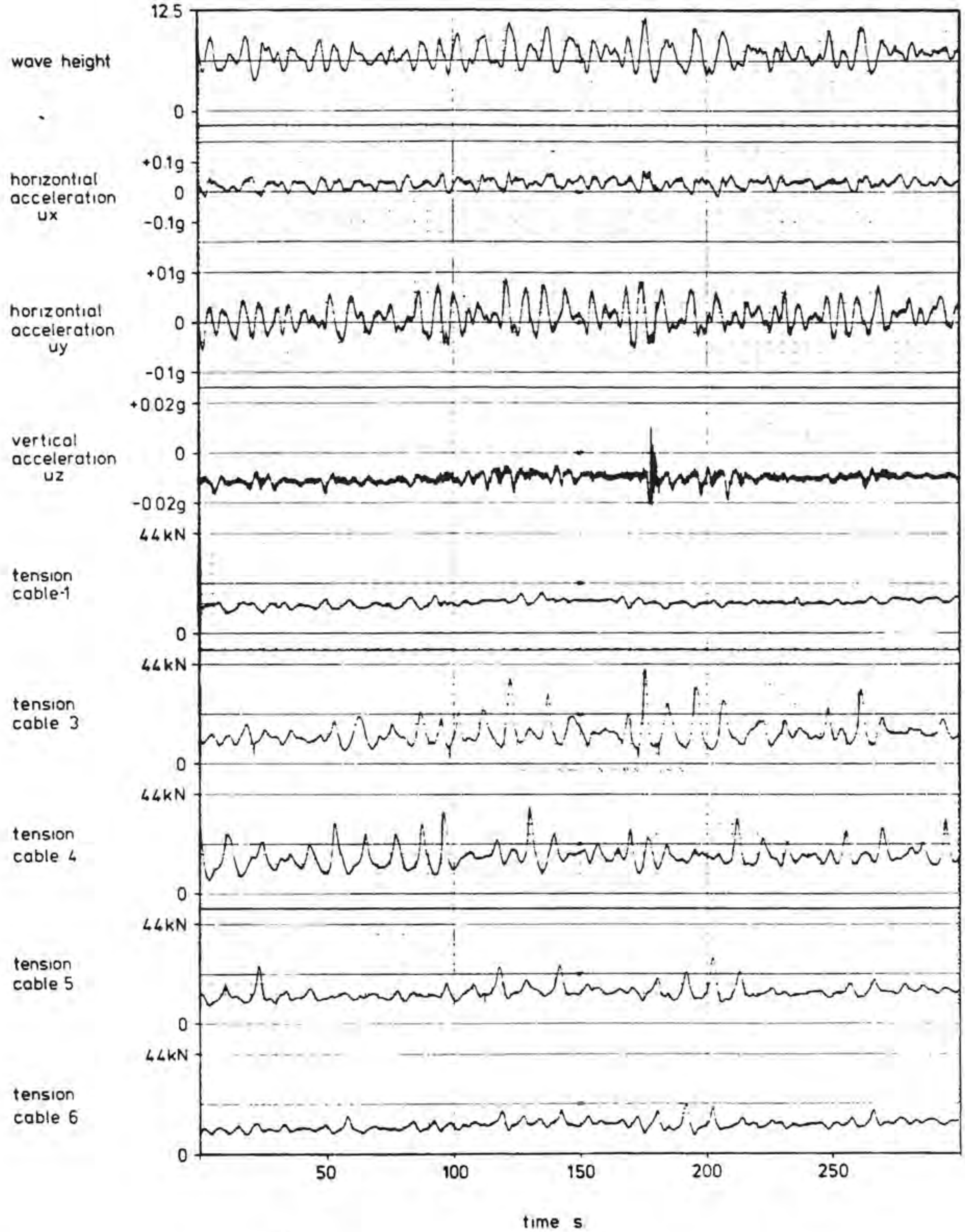

Fig. 4: Sample chart record - wave height, accelerations, cable tensions

event of a tilt of the tower combined with horizontal acceleration.

Strain gauge load cells were connected between each of the six upper mooring cables and the tower, so as to measure the in-line cable tension at the tower. Two ranges of measurement were available: 0-44 kN or 0-220 kN. This type of load cell had been found to work well in previous installations; however, the underwater electrical connectors used just below mean sea level proved to be unsatisfactory for the severe service conditions. The combination of submersion and wave action is thought to have deteriorated the seals of these connectors, thereby progressively reducing the number of load cells functioning at any one time. Load cells were not installed in the lower cables or the central mooring line because of associated installation and maintenance difficulties.

Description of collected data: Relevant data included wave height for all 192 runs, acceleration in three axes for 62 runs, and cable tensions for 30 engineering runs. As mentioned above, the tension measuring load cells were subject to failure and at best only five of the six load cells were functioning at any one time (Table 1).

The recorded data included RMS wave heights ranging from 0.3 m to 1.9 m with individual wave heights of 10 m recorded occasionally. RMS acceleration ranged from 0.08 m s^{-2} to 0.38 m s^{-2} in the horizontal direction. RMS cable tension ranged from 0.4 kN to 6.0 kN, with instantaneous tension exceeding the 44 kN range of recording in some instances. Fig. 4 illustrates a portion of the chart record obtained for wave height, acceleration and cable tension from one engineering run (Run #118). Similar records of 20 minute duration were analyzed, using the upward zero crossing technique (Mills, 1979) to develop bivariate histograms (scatter diagrams) of waveheight vs. wave

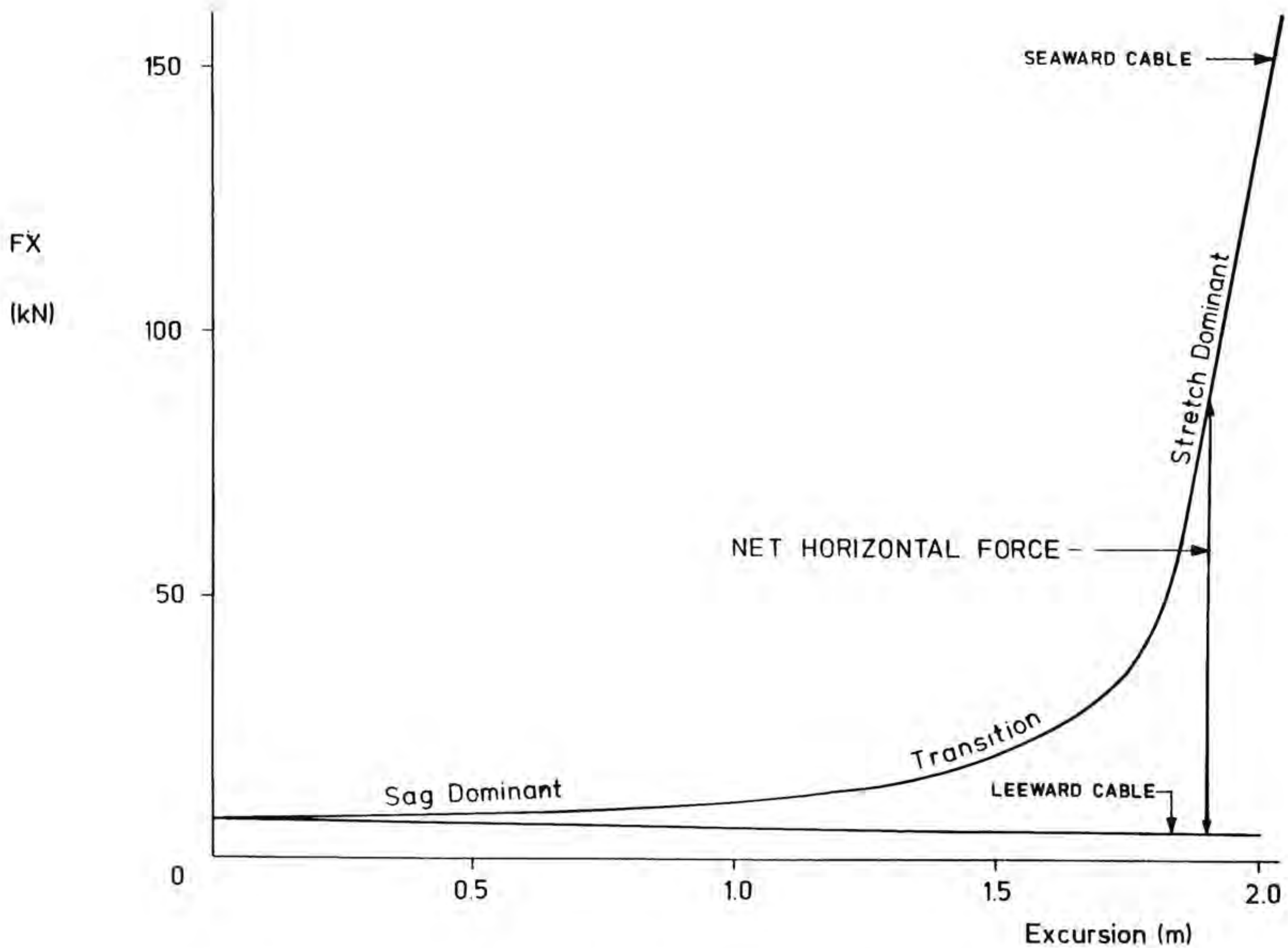

Fig. 5: Calculated horizontal load vs. excursion, upper cable pair

period and variation in cable tension vs. period, and used to obtain the mean, one-third largest and one-tenth largest occurrences.

Failure of the mooring system: During a severe storm in the second season of operation, failure of the shackles in the triple branch chain sling disconnected the base of the tower from the central mooring cable, leading to the breakage of several lower mooring cables and leaving the platform floating in a horizontal position. Although there was no structural damage to the tower, the project was terminated. During this storm, a 12 m high wave was recorded by a wave rider buoy located approximately 0.5 km from the platform site, which was recording data for 20 minutes every 3 hours. A maximum wave height for the storm of 15 m may be estimated from this data using the Rayleigh distribution. Data collected prior to the failure indicate that there was impulsive loading of the tower base and vertical movement of the tower prior to failure. Also, in subsequent testing, shackles similar to those which failed were found to have an ultimate strength approximately one half of that specified.

ANALYSIS OF PLATFORM MOTION

Static Analysis: The predicted displacement of the platform under static lateral loading is non-linear, both in magnitude and direction, because of the load/excursion characteristics of the mooring cables. The calculated relationship between horizontal displacement and the horizontal load resisted by a pair of opposite cables is highly non-linear, due to the transition from a sag-dominated condition in the cable under initial tension, to a stretch dominated condition of the seaward cable under extreme loading (Fig. 5). Also, when the load is applied to the tower at some angle between two adjacent cables (Fig. 6), the structure surges in the direction of the load until the more seaward cable approaches a stretch dominant, "bar tight", displacement

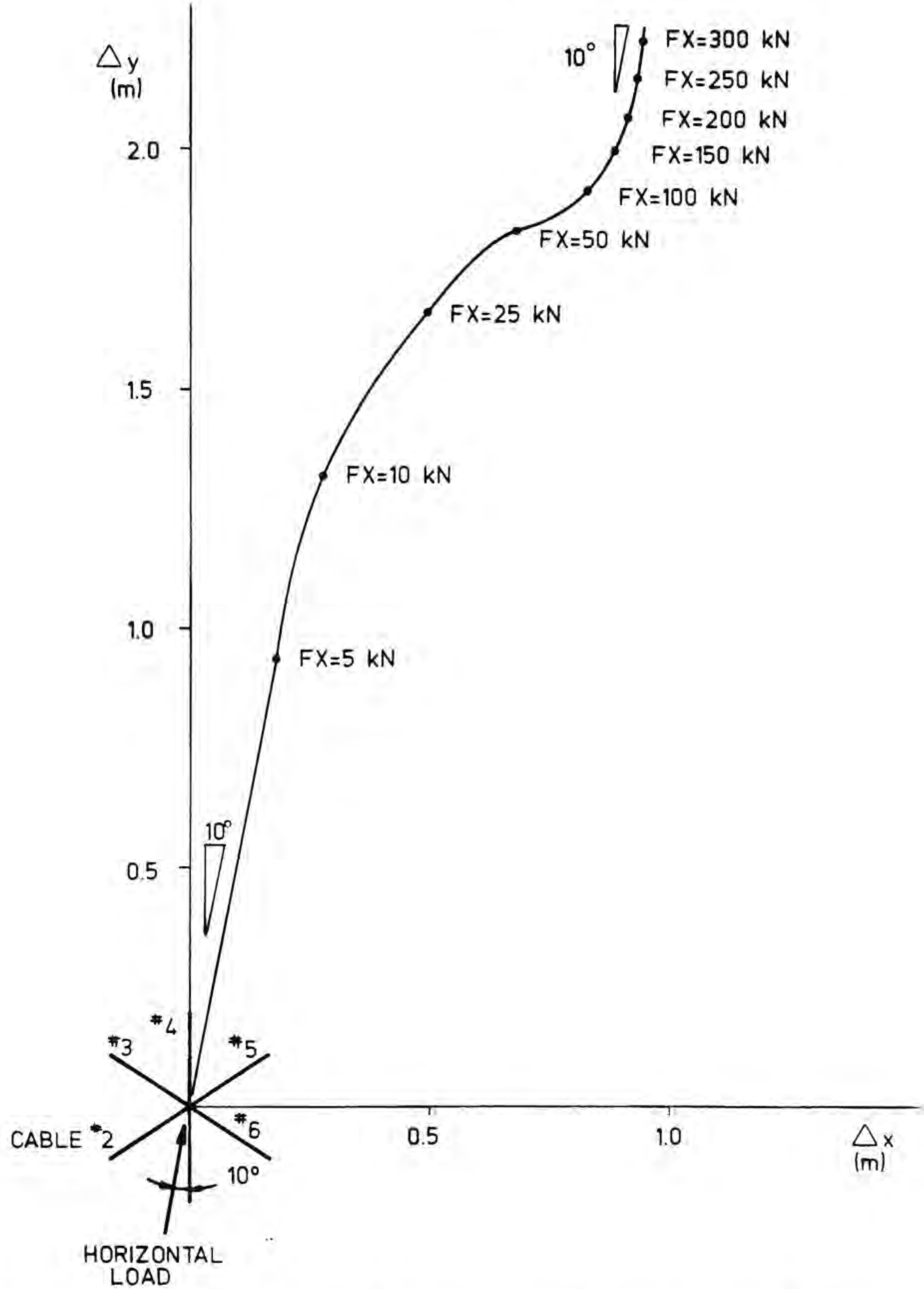

Fig. 6: Calculated displacement; variable load applied 10° from the axis of one cable

condition, then the tower sways as well as surges until the adjacent seaward cable also becomes "bar tight." This is followed by a more limited surge associated with the stretch of the two seaward cables, with the other four cables remaining in a relatively slack condition. The situation is further complicated by a possible tendency of the tower to yaw in order to reduce the sway caused by the non-linear excursion of the seaward cables. Horizontal load/displacement relationships (Fig. 7) have been calculated by Mills (1979) for various sea states using Morison's equation and linear wave theory. The relative significance of inertia and drag loading is indicated by the phase angle at peak displacement.

Dynamic Behaviour: Contrary to the phase relationships indicated in Figure 7, the chart records and results of the statistical analysis indicate a phase lag of between 0° to 30° in the tension of those cables estimated to be dominantly seaward, relative to passage of the wave crest. The phase lag is considered to be due to the dynamic response of the platform.

None of the chart records indicated a sympathetic resonance between wave loading and either acceleration or cable tension. Tension amplitudes invariably reduced to normal levels within one cycle of unusually large wave loading, due to the inherent damping of the system.

Shock Loading: During the second season, the chart records occasionally indicated sudden downward accelerations immediately following the passage of large waves (typically at wave heights of 9 m or greater with 10 s periods). The associated vertical movement may be attributed to a transient loss of tension in the central cable, due to the net buoyancy being exceeded by a combination of vertical wave loading and the vertical component of cable loads under horizontal loading of the tower. In many cases, the vertical movement was associated with large oscilla-

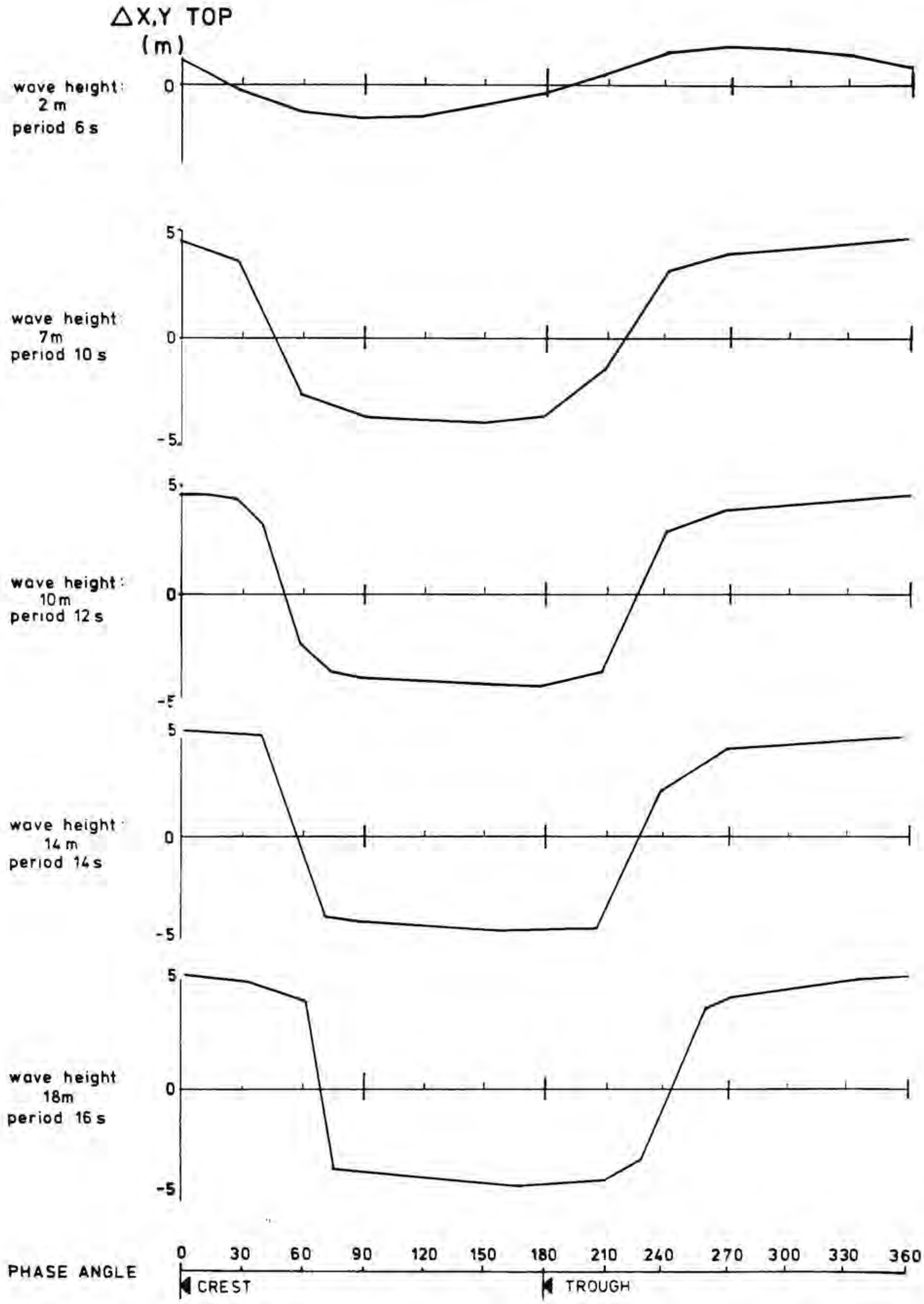

Fig. 7: Calculated static response to loading - horizontal movement at top vs. phase angle (Mills, 1979)

tions in the vertical and horizontal axes at frequencies of 1.5 Hz and 2.5 Hz respectively, and minor oscillations in the mooring cable tensions at 0.8 Hz (Fig. 8). The frequency of vertical oscillation was consistent with that for the mass-spring system formed by the tower and the central cable, and is considered to be driven by the impact of the tower on the central cable as the tower returned to its original position. Maximum accelerations in the order of 0.1 g to 0.2 g were extrapolated from the chart records, indicating that the central cable experienced impulsive loads in the 50 kN range.

Where tension measurements were taken during shock loading of the tower, the sum of in-line tensions of the six upper cables was estimated to be approximately 150 kN. By the analysis described in Appendix A, this indicates a net horizontal load resistance of 78 kN in the upper cables. A vertical hydrodynamic force of 60 kN would then be required to overcome the remaining tension in the central mooring cable. By applying Morison's equation and assuming that these forces occur simultaneously at peak horizontal particle velocity and peak vertical acceleration, a horizontal drag coefficient of $C_d = 0.94$ and equivalent vertical inertia coefficient of 1.5 are derived for 9 m, 10 s waves.

It was also noted that, with cable tensions measured in the 0-220 kN range, the sum of upper cable tensions did not exceed 150 kN for waves considerably larger than those required to cause shock loading of the platform. The movement of the platform provided an upper limit to cable tension during the passage of these waves, and the value of this upper limit is associated with the platform's buoyancy.

<u>Monitoring of the platform's performance:</u> The effect of platform acceleration on scientific data has been examined using co-spectral statistics (Smith, 1980a). Also, a record was maintained of

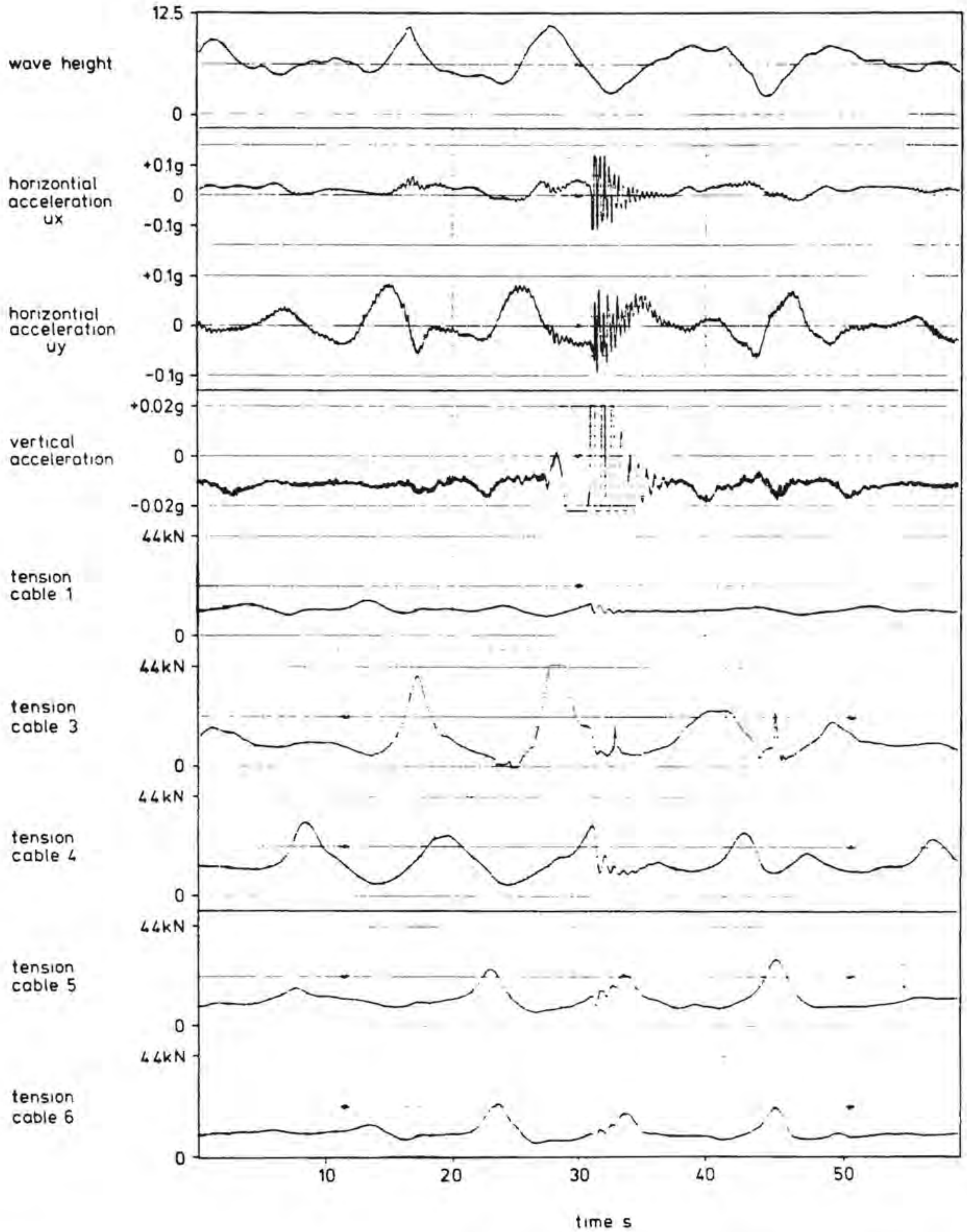

Fig. 8: Chart record of shock loading event - wave height, accelerations, cable tensions

the ratio of RMS horizontal acceleration at the instrument level to RMS wave height, so as to detect any deterioration in structural performance. The significance of this information was illustrated by a 40% reduction in acceleration following the tightening of cables in the summer of 1977 (Fig. 9); however, there was no noticeable increase in acceleration toward the end of the second season to suggest any yield in the cables or shifting of the anchors prior to the time of failure. RMS acceleration in the horizontal plane was found to be generally proportional to wave height for a given wave period. However, waves with longer periods, which tended to be associated with larger waves, had smaller ratios of acceleration to wave height. To obtain a relationship between the characteristic frequency and the acceleration-to-wave height ratio, the RMS horizontal acceleration (Table 1) was calculated using the two components $\dot{u}_x$ and $\dot{u}_y$ as below:

$$(\dot{u})_{RMS}^2 \approx [(\dot{u}_x)_{RMS}^2 + (\dot{u}_y)_{RMS}^2] \qquad (2)$$

Forty runs in the second season were grouped by the frequency band at the peak of their respective wave spectra. The average ratio of acceleration to wave height was calculated for each group. A least squares analysis of the acceleration to wave height ratio versus the frequency band, weighted by the number of recordings in each band, provided the following relationship for horizontal acceleration at the tower top:

$$\dot{u}_{RMS}/H_{RMS} = 0.50\ f_o^{0.43} \qquad (3)$$

with a probable error of 10% in the mean value for each of the eight (8) frequency groups. Individual recordings, however, had a considerable distribution about the mean acceleration-to-wave height ratio for each frequency group.

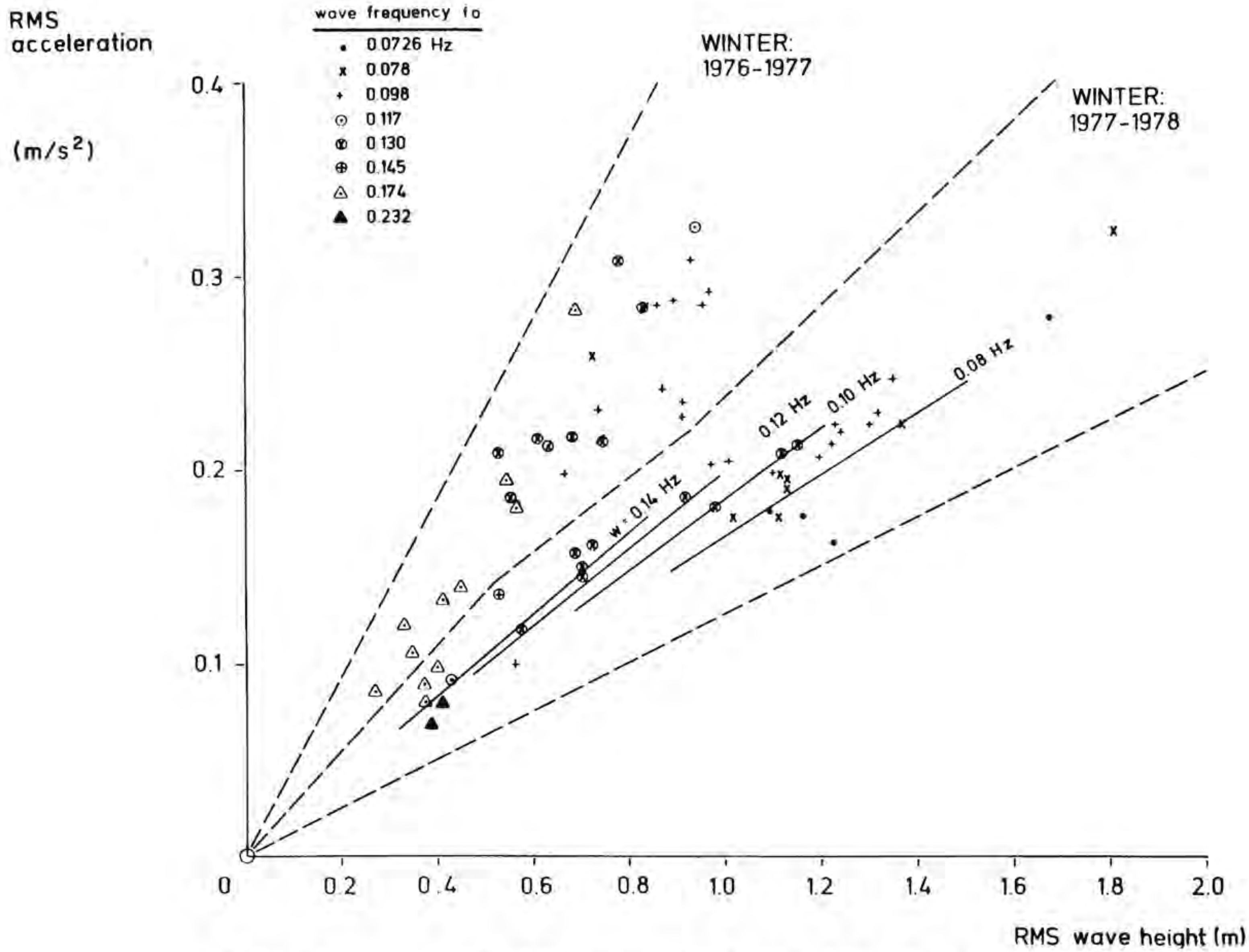

Fig. 9: RMS acceleration at the top of the tower vs. RMS wave height, sorted by peak frequency of wave spectrum

ANALYSIS OF WAVE LOADING DATA

The data were used to: a) investigate the relationship between wave height and loading in terms of Morison's equation, b) compare RMS, significant and one-tenth largest wave height data with their respective response amplitudes, and c) relate measured wave spectra and response spectra for cable tension.

Numerous variables affected the tension in each of the upper cables: initial tension, dominant wave direction, the extent of deviation about the dominant wave direction, current velocity and direction, wind velocity and direction, the distribution of horizontal load between upper and lower cables and the central mooring cable, tidal elevation, dynamic effects and, of course, the wave height and period. These were examined for their impact on the accuracy of any wave height and force relationship to be derived from the data. A static, non-linear analysis was used for this examination, with hydrodynamic loads calculated using Morison's equation and linear wave theory.

1) A one meter reduction in mean sea elevation was found to reduce drag forces by 0.4% and increase inertia forces by 2.8% for waves with a period of 10 sec. The effect of tidal variation (approximately +0.9 m about MSL) was therefore disregarded.

2) The maximum mean wind speed recorded during any engineering run was 19 m/s, which results in 4.0 kN loading on the tower. The corresponding maximum mean tension in any of the upper cables was 15.3 kN, and wind pressure was therefore significant to the mean tension of individual cables. However the variation in wind pressure and direction were small and at a different frequency to wave loading, and could be disregarded when relating wave height to cyclical variations in wave loading of the tower.

3) When added directly to wave induced particle velocity, the design current would contribute significantly to the maximum force on individual cables and on the tower as a whole. A current velocity in the direction of a wave stream increases hydrodynamic drag during the passage of a wave crest, and reduces the drag force in the opposite direction at the wave trough. The variation in hydrodynamic drag due to current is non-linear, due both to the force/particle velocity relationship and to there being a greater area of the tower exposed to the wave crest than to the wave trough. The presence of a current would therefore affect both the mean force acting on the tower and, to a lesser extent, the magnitude of variation about the mean. For example, for a wave period of 10 seconds, a design current of 0.25 m s^{-1} increases the maximum horizontal force on the platform by 40% for wave heights of 4 m, and by 30% for wave heights of 7 m. However, the corresponding increase in the variation of horizontal force over a wave cycle would be 10% and 7% respectively. Peak-to-trough and RMS variations were therefore used in the data analysis.

4) It was found that, in the case of 4 m waves with a period of 10 s, the calculated maximum drag force on the structure was 13% greater when the wave theory was applied to the peak of the wave crest than when wave loading was considered at and below the mean sea level only. A corresponding increase of 23.5% was found for 7 m waves. However, for both wave heights, the maximum variation in calculated drag force over a wave cycle was only 1% greater when calculated by loading the tower to the crest in one direction and to the trough elevation in the opposite direction, than when calculated to the mean sea level in both directions.

5) The tower's flexibility was minimal in relation to that of the cable mooring system. The tower could therefore be

considered as totally rigid, and the distribution of loads into the mooring system could be derived directly from the load-displacement characteristics of the cables.

6) When the bottom of the tower is displaced, the tension in the central cable has a horizontal component which we will consider here. Given a totally rigid tower, a horizontal loading profile and the concurrent vertical load, the cable system could be resolved to relate loading of each cable connection to the total horizontal force. However, the vertical component of wave drag loading was unknown and, as indicated by the shock loading observation, may have been quite large. For a 7 m, 10 s wave, using $C_d = 1.0$ and $C_m = 1.5$ and considering no ballast in the buoyancy tanks and no hydrodynamic vertical loads, the calculated peak horizontal load of 71.8 kN would be distributed as follows: 43.9 kN to the upper cables, 17.5 kN to the lower cables and 10.4 kN to the central cable. The horizontal load resisted by the central cable is primarily a function of its tension (157 kN) and horizontal displacement (1.22 m). If the horizontal load carried by the central cable is neglected, the 71.8 kN horizontal load would be distributed as 47.0 kN to the upper cables and 24.8 kN to the lower cables: that is, the upper cable reaction would increase by 7.1%. A corresponding increase for a 10 m, 12 s wave would be 1.6%. With the tanks ballasted as measured during recovery, the net buoyancy of 137 kN provided a central cable tension of 95 kN at rest. Under this ballast and a 2 m, 6 s wave, the assumption of no reaction to horizontal load from the central cable would result in an over-estimate in the upper cable reaction of 19%. This figure would, however, be reduced by concurrent vertical loads and any damping of the central cable displacement.

Oscillograph recordings were analysed to relate wave height and horizontal load at the upper cable connection (Appendix A).

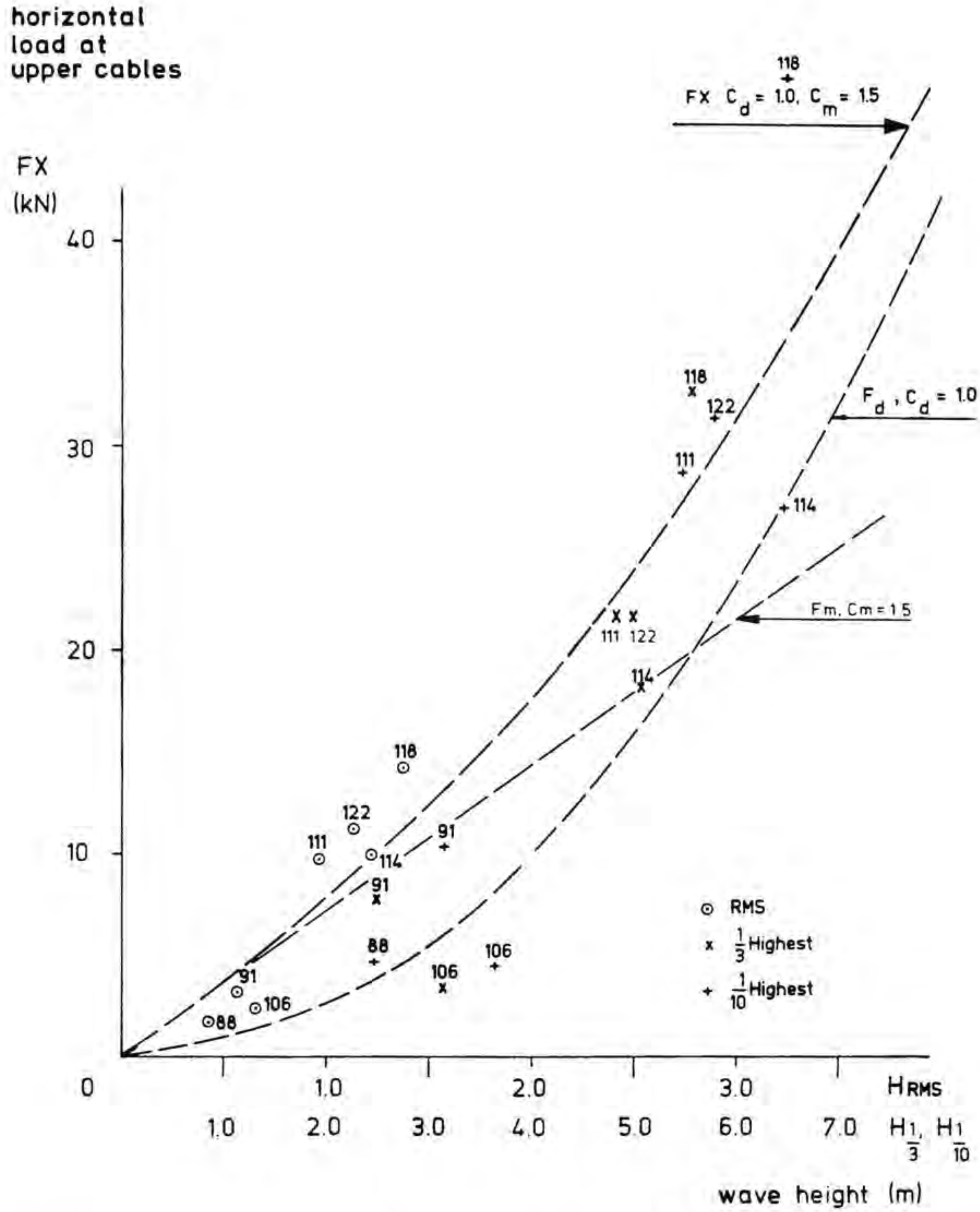

Fig. 10: Horizontal loading of upper cable connection vs. wave height, calculated for 10 s wave period using measured cable tensions

Wave height and cable tension were averaged over a number of load cycles (typically a 20 minute period). The influence of forces that did not oscillate at or near the peak wave frequency was minimized by considering only the variations in each cable tension that occur in the wave frequency range. The influence of wave direction was minimized by relating wave height to a scalar value for net horizontal force at the upper cable connection. The effect of horizontal force at the central cable was disregarded. The calculated drag and inertia forces acting on the upper cable connection were then examined independently to assess the influence of wave period and to standardize the measured results at a characteristic wave period of 10 seconds.

The horizontal forces at the upper cable connection, as derived from the cable tension data, are plotted against measured wave height in Fig. 10. The graph presents RMS, one-third largest and one-tenth largest values from the seven engineering runs listed in Table 2. The reference curves indicated are of FX, F_d and F_m as calculated for C_d = 1.0 and C_m = 1.5. Because H_{RMS} expresses sea-state in terms of wave amplitude (one half of peak-to-trough wave height), whereas $H_{1/3}$ and $H_{1/10}$ express sea-state in terms of peak-to-trough wave height, two abscissa scales are required in Fig. 10 for direct comparison of RMS and peak-to-trough values.

With the exception of Run Nos. 111 and 122, the RMS, one-third and one-tenth largest values for each data run were generally consistent in their relation to the line calculated for C_d = 1.0 and C_m = 1.5. Because of the 90° phase angle between inertia and drag loads, the maximum horizontal force is relatively independent of the inertia load for wave heights greater than 6 m and independent of the drag load for waves less than 4 m.

For smaller wave heights and shorter wave periods, measured forces were less than those calculated by Morison's equation and

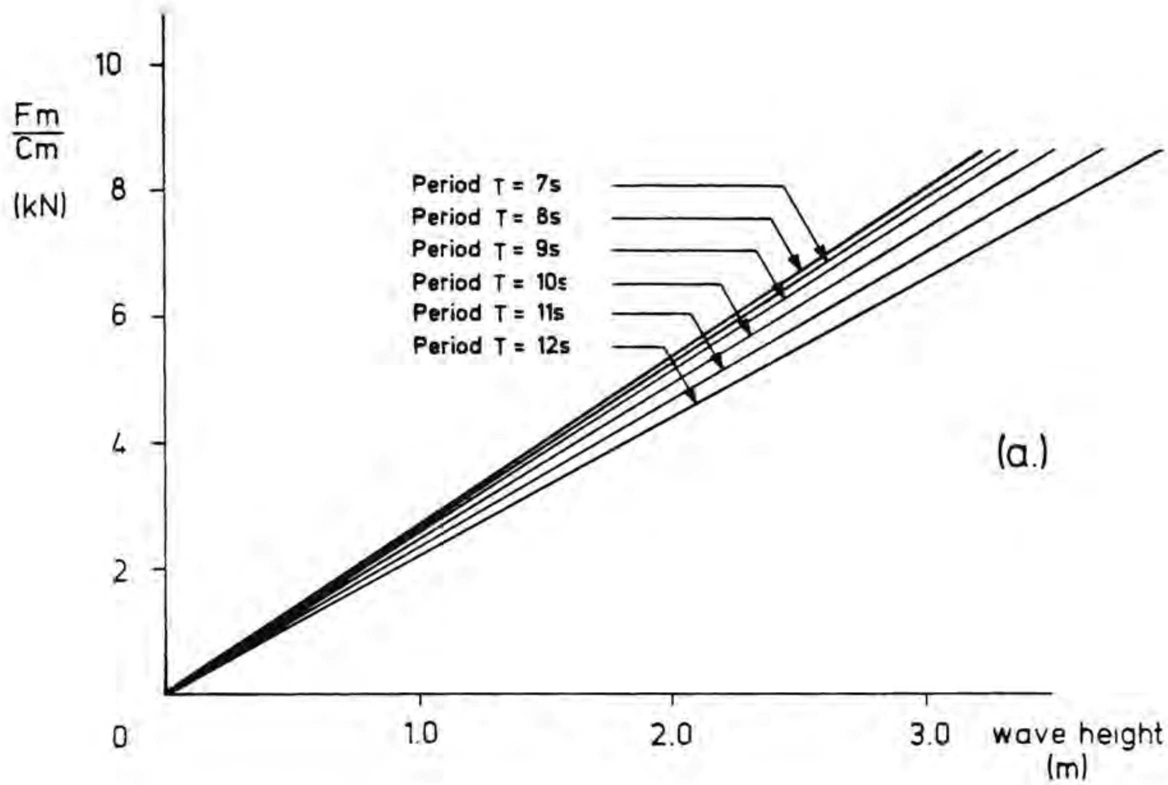

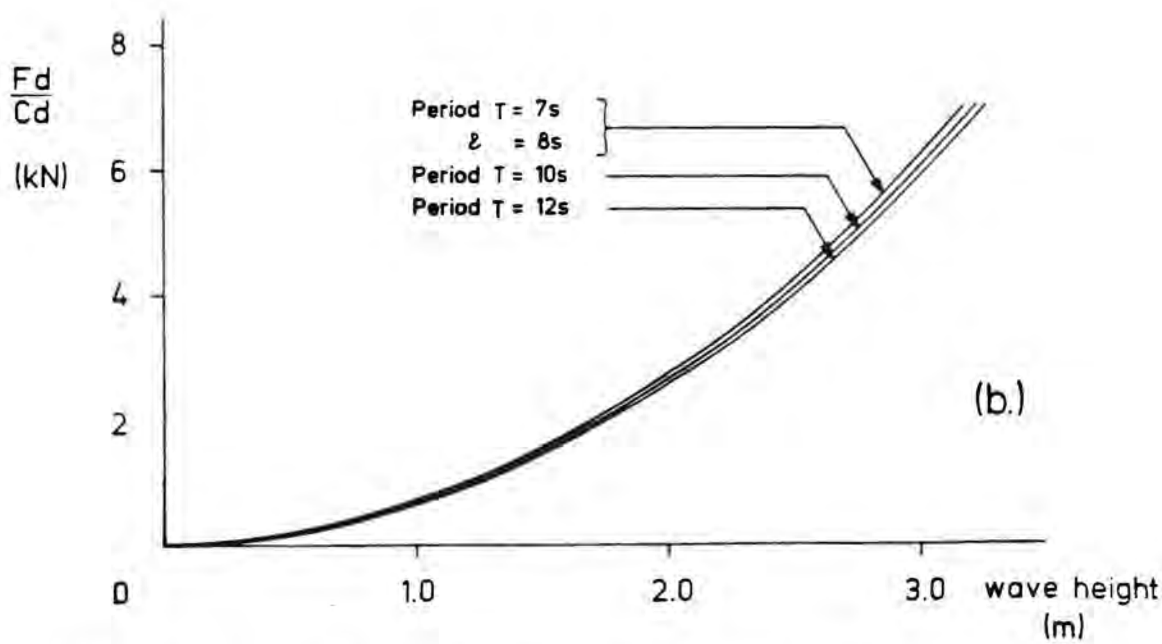

Fig. 11: Maximum force components vs. wave height,
(a) inertia force / coef. of inertia
(b) drag force / coef. of drag

linear wave theory. This is consistent with the increased influence of the central mooring cable on upper cable forces at smaller wave heights. Also, it appears that the cables did not develop their full static load due to damping of the structure within the sag dominated loading regime.

As shown in Fig. 11, both the drag force and inertia force calculated for the upper cable connection are quite uniform for wave periods ranging from 7 s to 12 s. The response amplitude operator (RAO) would therefore show little variation over this range of wave period, given constant values for C_d and C_m. While a spectral analysis of the horizontal force at the upper cable connection was not derived from the cable tension data, the wave height and individual cable tension spectra were very similar for all engineering runs analyzed: this is consistent with a uniform RAO for horizontal force on the platform.

DISCUSSION AND CONCLUSION

Possible modifications of mooring: If a similar structure were installed in the future, modifications would be made in view of past experience. Synthetic materials such as Kevlar which have stretch characteristics comparable to steel would be considered for the mooring cables since their near-neutral buoyancy would require less pre-tension and would virtually eliminate catenary sag, making the mooring much stiffer. Less water ballast would be used; and the increased net buoyancy, in conjunction with reduced motion in response to waves, would raise the threshold for the onset of shock-loading events caused by a temporary loss of tension in the central cable. An added advantage of synthetic materials is corrosion resistance. However, drag on the cables themselves would have to be considered due to their larger diameter for comparable strength. A means of providing damping to reduce impact loads would also require investigation.

Conclusion: The engineering data obtained from the platform was limited to peak-to-trough wave heights in the order of 9 m and therefore cannot be extended to the design requirements for the tower with any great certainty. However, analysis of the data indicated that:

- the maximum loading of this structure is, for all practical purposes, entirely due to drag forces, as opposed to inertial forces;

- using linear wave theory, a coefficient of drag C_d, of 1.0 and a coefficient of inertia C_m, of 1.5 are consistent with data obtained at wave heights of up to 9 m;

- for the calculation of maximum loads, static design methods and linear wave theory are adequate for structures of similar dimension and stiffness. However the dynamic response of the tower was found to significantly reduce the cable loading associated with small, short-period waves;

- displacement due to waves was dependent on the initial tension in the mooring cables, which determined the magnitude of the non-linear transition zone from sag-dominated to stretch-dominated displacements. An increase in cable tension and in buoyancy would have greatly reduced lateral movement of the tower;

- acceleration and velocity of the tower due to wave loading were significantly different from predictions by static calculations (Fig. 7) due to the inertia of the structure and its mooring cables;

- failure was caused by the shock loading of the central mooring cable, brought about by the loss of tension when the tower was subjected to severe wave loading, and by components which were later found to be defective and to have a smaller safety factor than called for in the design of the mooring system.

APPENDIX 'A'

Relationship Between Measured Wave Height and Cable Tension

Data Used: An estimate of tension in all six upper cables was required to obtain scalar (non-directional) results for force. Had load cell measurements been available for all six cables, the recordings could have been processed to provide the horizontal and vertical force at the upper cable connection. However, with at best only five load cells operating, it was not possible to calculate these forces without first estimating the tension in those cables for which data were not available. RMS tensions in those cables were estimated using the recorded RMS values for the remaining cables, together with an estimate of the predominent wave direction based on wind azimuth, acceleration data and correlation coefficients. Unfortunately, the cables with malfunctioning load cells were frequently oriented close to the direction of predominant wave loading. Only seven of the engineering runs made in the second season, each with one load cell not recording, yielded an uncertainty of less than 10% in the estimated sum of RMS tension in all six cables. The analysis was therefore confined to these seven runs, for which wave height and period characteristics are given in Table 2.

Averaging of Data: The wave characteristics of most interest in design are the profile, period, and height distribution of larger-than-average waves. The "significant wave height" of a sample, that is the average of the one-third largest wave heights, is commonly used for reference, and was used in this analysis. The average of the one-third largest variations in tension was obtained for each cable with an operable load cell, and their sum was prorated with RMS tension to estimate the tension in the cable with the malfunctioning load cell. One-tenth largest wave and tension data were also obtained for comparison with one-third largest data.

Table 2: Wave height and period of RMS, one-third and one-tenth largest waves for analyzed engineering runs.

Run	Wave height (m)				Period (s)			
	RMS	Mean	1/3	1/10	fo	Mean	1/3	1/10
88	0.44	1.44	2.08	2.48	8.6	6.98	7.33	7.14
91	0.56	1.76	2.49	3.18	10.2	8.33	9.92	10.27
106	0.66	2.20	3.06	3.68	--	6.67	6.69	6.62
111	0.96	3.64	4.57	5.43	--	9.86	9.00	8.77
114	1.22	3.43	5.06	6.42	10.2	8.48	9.18	9.69
118	1.37	3.68	5.56	6.40	12.8	8.19	9.87	9.69
122	1.14	3.02	4.65	5.75	12.8	8.43	10.80	10.64

Statistical results (RMS wave heights and RMS tensions) relate all fluctuations in cable tension to all wave heights over the entire period of record, whereas "significant" wave height and "significant" tension data are derived on the basis of the onethird of the record containing the largest fluctuations. Furthermore, the "significant" fluctuations in cable tension do not necessarily occur in every case in response to the passage of the "significant" wave heights. Accordingly, RMS wave height and force relationships were developed for comparison with "significant" values.

Isolation of Wave Induced Loads: As illustrated in Fig. 5, an applied horizontal load is resisted by the difference in the horizontal loads acting on opposite cables. Any change in applied load is equal to the vector sum of the changes in the cable loads: for instance, the increase in an applied horizontal load would equal the increase in the horizontal component of loading of the seaward cable plus the horizontal component of load reduction in the leeward cable and, similarly, the magnitude of a reduction in applied load would equal the magnitude of reduction in loading of the seaward cable plus the increase in loading of the leeward cable. Therefore, over a complete wave cycle, the sum of forces associated with the wave crest in one direction and the wave trough in the opposite direction is represented by the sum of the vector component of variation in each cable tension, as resolved in the direction of the wave.

Wave Induced Loading of the Upper Cable Connection: To obtain values for the net horizontal load on the upper cable connection from averaged values of the variation in each cable tension, it is necessary to: 1) resolve the horizontal component of tension in each cable, and 2) relate the horizontal forces to the net horizontal load on the tower. Both these relationships are non-linear, but linear approximations were considered reasonable in relation to the probable error introduced by having tension data from only five of the six upper cables. Results obtained using linear approximations were found to be within 4% of those results obtained by iterative solution of the non-linear computer model developed by Mills (1979).

1) To resolve the horizontal components, FX_i, of the measured tensions, FT_i, the following ratios of tension to horizontal load were calculated from the angle of catenary at the upper end of any upper cable "i":

$$
\begin{aligned}
FT_i/FX_i &= 1.28 \text{ at } -2.5 \text{ m excursion} \\
&= 1.25 \text{ at } 0.0 \text{ m excursion} \\
&= 1.14 \text{ at } 1.0 \text{ m excursion} \\
&= 1.06 \text{ at } 2.5 \text{ m excursion}
\end{aligned}
$$

The approximations used for this analysis were based on the sum of cable tensions and allowed for a typical range of excursions:

RMS wave heights: $\sum FT_i / \sum FX_i = 1.20$

1/3 largest waves: $\sum FT_i / \sum FX_i = 1.15$

1/10 largest waves: $\sum FT_i / \sum FX_i = 1.10$

2) To relate the horizontal loads on the cables, FX_i, to the net horizontal load on the upper cable connection, FX, it is necessary to consider the transition from a system of all three pairs of opposite cables resisting nominal horizontal loads in the sag-dominated regime, to a system of one or two cables resisting large loads. For small or moderate wave loads, the system was analyzed as a linear - elastic model of three pairs of opposite cables. The angle of wave attack was varied in 5° increments to obtain an average ratio of FX to FX_i for any angle of attack:

$$\sum_{i=4}^{6} \left| FX_i - FX_{(i-3)} \right| \simeq 1.28\ FX \text{ (range 1.15 to 1.33)}$$

Similarly, the case of large wave loading was analyzed as a linear-elastic model of two adjacent cables only:

$$\sum_{i=4}^{6} \left| FX_i - FX_{(i-3)} \right| \simeq 1.10\ FX \text{ (range 1.0 to 1.16)}$$

The approximations used for the structural analysis were chosen by considering the loading of the most seaward cable tension, as illustrated in Fig. 5:

$$\left(FX_i\right)_{MAX} \leq 20\text{ kN:} \quad \sum_{i=4}^{6} \left| FX_i - FX_{(i-3)} \right| = 1.28\ FX$$

$$\left(FX_i\right)_{MAX} \geq 60\text{ kN:} \quad \sum_{i=4}^{6} \left| FX_i - FX_{(i-3)} \right| = 1.10\ FX$$

A linear transition was approximated between the two models.

Horizontal Load for a Uniform Wave Period: The effect of wave period on the drag force component, F_d, and the inertia force component, F_m, was examined using linear wave theory (Bretschneider 1969), for which the horizontal components of velocity and acceleration are:

$$v = a\omega . \frac{\cosh k(z+d)}{\sinh kd} . \sin(kx - \omega t) \quad (4)$$

$$\dot{v} = a\omega^2 . \frac{\cosh k(z+d)}{\sinh kd} . \cos(kx - \omega t)$$

Peak values for each term were applied to obtain the peak in each of the force components in Morison's equation:

$$F_d = 1/2 \rho C_d Av|v| : \quad = a\omega . \frac{\cosh k(z+d)}{\sinh kd} \quad (5)$$

$$F_m = \rho C_m V \dot{v} : \quad \dot{v} = a\omega^2 . \frac{\cosh k(z+d)}{\sinh kd}$$

To isolate the effect of wave period, the force components acting on the upper cables were considered as a function of the coefficients C_d and C_m, amplitude, a, and frequency - dependent terms, D_o and M_o:

(6)

$$F_d = C_d a^2 D_o \text{ where } D_o = \frac{\rho \omega^2}{2 L_u \sinh kd} . \int_{-d}^{0} \cosh^2 k(z+d).A(L_L+z).dz$$

$$F_m = C_m a M_o \text{ where } M_o = \frac{\rho \omega^2}{L_u \sinh kd} \int_{-d}^{0} \cosh k(z+d).V.(L_L+z).dz$$

where A and V are functions of z. D_o and M_o were then solved numerically for various wave periods over the range of recorded values, with the tower modelled as seven discrete vertical elements. As shown in Fig. 11, wave period had a greater influence on inertia forces than on drag forces for small wave heights, which is where inertia forces dominate, and both inertia and drag forces on the upper cable connection were greatest for wave periods in the 7-8 s range. The approximation used for analysis was that FX be factored by the ratio of M_o for a 10 s period to M_o for the measured period when the measured wave height

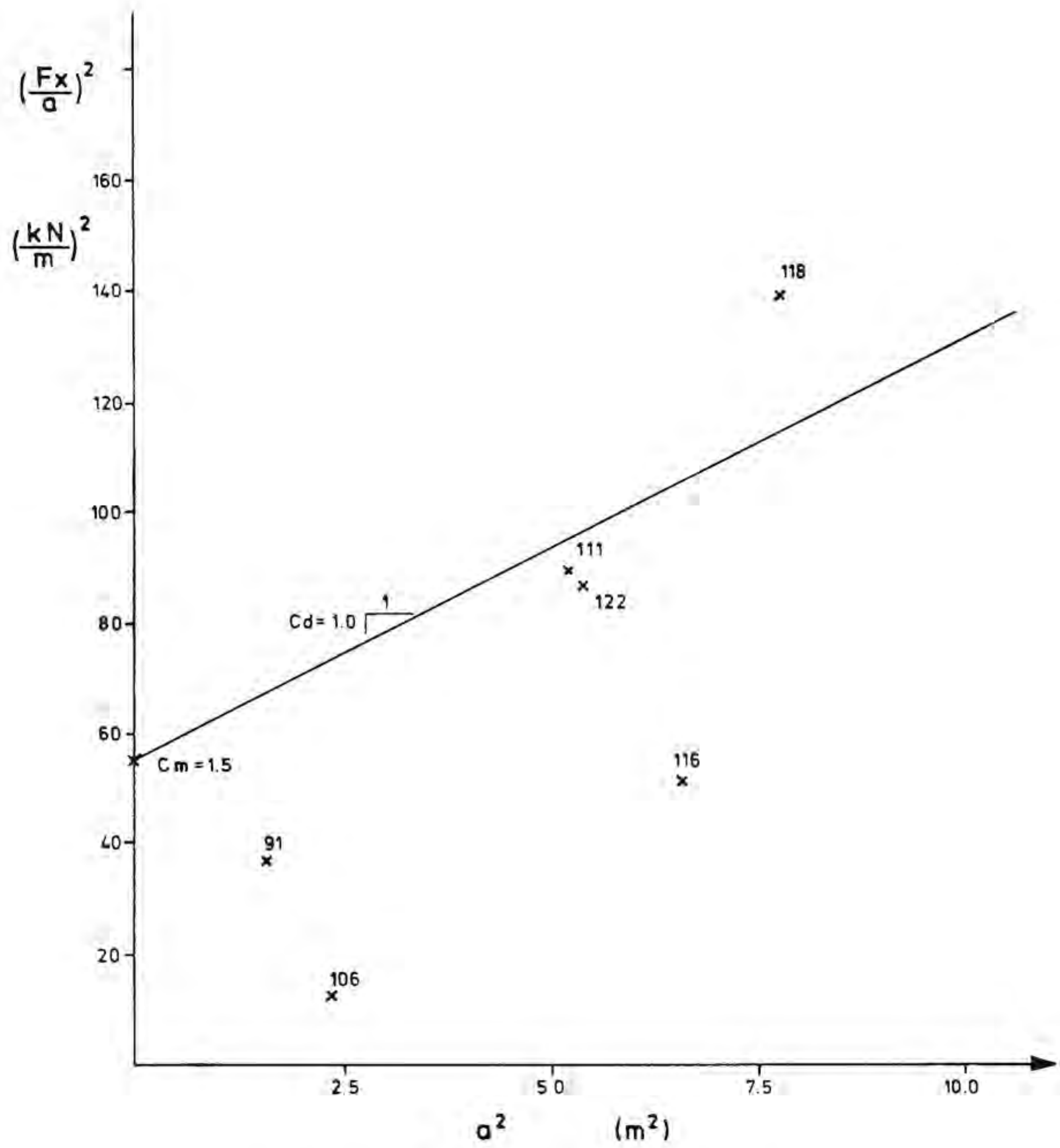

Fig. 12 Straight line fit of data for C_d and C_m: one-third largest waves, adjusted for 10 s wave period.

was less than 4 m, and that a corresponding ratio using D_o be used for larger wave heights. The uncertainty in results created by this arbitrary method was considered to be less than 5% over the range of values for C_d and C_m reported in the literature.

Fig. 10 shows the horizontal force at the upper cable connection, plotted against wave height, for a 10 s wave period as derived from seven engineering runs. Using linear wave theory and disregarding the tower's dynamic behaviour, values for C_d and C_m may be estimated by a curve fit using measured horizontal force and wave amplitude and calculated values for D_o and M_o. Because of the sine and cosine - dependent terms in the drag and inertia forces, the maximum horizontal force is obtained by the quadratic addition of the peak values of the component forces.

$$(7)$$

$$FX^2 = F_x{}^2 + F_m{}^2$$

$$= (C_d.a^2.D_o)^2 + (C_m.a.M_o)^2$$

Then $(FX/a)^2 = (D_o.C_d)^2.a^2 + (M_o.C_m)^2$

C_d and C_m would then be obtained by plotting $(FX/a)^2$ vs a^2 (Fig.12).

NOTATION

A	cross-sectional area of exposed surface
a	wave amplitude = 1/2 H
C_d	drag coefficient
C_m	inertia coefficient
D	width of structure
d	mean water depth
FT_i	in line tension in cable "i" at connection to structure
FX	horizontal force applied to upper cables
FX_i	horizontal component of tension in cable "i"
F_d	drag force applied to upper cables
F_m	inertia force applied to upper cables
f_o	frequency at peak of wave spectrum
g	gravitational acceleration
H	wave height, peak-to-trough
K	Keulegan - Carpenter Number
k	wave number = $2\pi/L$
L	wave length
L_L	distance from lower cables to sea level at rest
L_u	moment arm of upper cables about lower cables
R_e	Reynold's Number
T	wave period
u	horizontal velocity of top of tower
V	displaced volume
v	horizontal water particle velocity
$\dot{v}$	horizontal water particle acceleration
x, y	cartesian co-ordinates
z	elevation with respect to sea level at rest
ν	kinematic viscosity
ρ	mass density of fluid
ω	wave frequency (rad/sec)

References

Bretschneider, C.L. 1969, Water Loads on Fixed, Rigid Marine Structures. Handbook of Ocean and Underwater Engineering, Myers, Holm, and McAlister, ed., McGraw-Hill/North American Rockwell Corp. 12.24 - 12.56.

Chakrabarti, S.K. 1982. Wave Force Coefficients for Rough Vertical Cylinders. Journal of Americian Society for Civil Engineering, Vol. 108, No. WW4, 445-455.

Dessureault, J.-G. and Knox, D.F. 1980. Design of a tri-axial thrust anemometer for measurement of atmospheric turbulence over water. Ocean Engineering, 7, 521-537.

Dinn, D.F. 1973. A remote-controlled, multi-channel, analog-data telemetry system. Rep. No. 73-11, Bedford Institute of Oceanography, 118p. *

Dobson, F.W., Brown, R.F. and Chang, D.R. 1974. A set of programs for analysis of time series data including fast Fourier transform spectral analysis. Computer Note 74-2, Bedford Institute of Oceanography, 334 pp. *

Doe, L.A.E. and Brooke, J. 1965. A Moored Stable Platform for Air-Sea Interaction Studies. Limnology and Oceanography, 10, R79-R86.

Hogben, N., Miller, B.L., Searle, J.W. and Ward, G. 1977. Estimation of Fluid Loading on Offshore Structures. National Maritime Institute, Rep. 11, April 1977.

Leonard, J.W., Garrison, C.J. and Hudspeth, R. T 1981. Deterministic Fluid Forces on Structures: A Review. American Society for Civil Engineering Vol. 107, No. ST6, 1041-1057.

Mills, R.G. 1972. Design and Installation of the Atlantic Oceanographic Laboratory Stable Platform. Rep. 72-4, Bedford Institute of Oceanography, 72 p. *

Mills, R.G. 1979. Non-Linear Response of Cable Supported Strucures to Wave Loading. M. Eng. Thesis, Dept. of Civil Engineering, University of Liverpool, 112p.

Morison, J.R., O'Brien, M.P., Johnson, J.W. and Shaaf, S.A. 1950. The Force Exerted by Surface Waves on Piles. Trans., American Institute of Mining, Metallurgical and Petroleum Engineers, Vol. 189, 149-154.

Neu, H.J.A. 1971. Wave Climate Study of the Canadian Atlantic Coast and Continental Shelf, 1970. Rep. 1971-10, Atlantic Oceanographic Laboratory, 103 p. *

Neu, H.J.A. 1982. 11-year deep water climate of Canadian Atlantic waters. Can. Tech. Rep. Hydrogr. Ocean Sci. 13, vii + 41 p. *

Skjelbreia, L. 1959. Gravity Waves, Stokes' Third Order Approximation, Tables of Functions. The Engineering Foundation Council on Wave Research, California Research Foundation, Berkley, Calif., 337 p.

Smith, S.D. 1974. Program A to D for analog-to-digital conversion and processing of time series data. Computer note 74-1, Bedford Institute of Oceanography, 68 p. *

Smith, S.D. 1980a. Evaluation of the Mark 8 Thrust Anemometer - Thermometer for Measurement of Boundary Layer Turbulence. Boundary-Layer Meteorol., 19, 273-292.

Smith, S.D. 1980b. Wind Stress and Heat Flux over the Ocean in Gale Force Winds. J. Phys. Oceanogr., 10, 709-726.

Smith, S.D. 1980c. Dynamic Anemometers. In: Instruments and Methods in Air-Sea Interaction. F.W. Dobson, L. Hasse and R. Davis, Eds, Plenum Publishing Corp, 65-80.

* Available in microfiche.